Publisher homepage: www.universepg.com, ISSN: 2707-4625 (Online) & 2707-4617 (Print)
https://doi.org/10.34104/ijmms.020.016028
International Journal of Material and Mathematical Sciences
Journal homepage: www.universepg.com/journal/ijmms

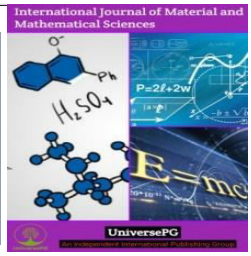


# First Principles Study of Structural, Elastic, Electronic and Optical Features of the Non-centrosymmetric Superconductors $SrMGe_3$ (Where M= Ir, Pt, and Pd)

**Mst. Jannatul Naefa[1], and Md. Atikur Rahman[2]***

[1&2]Department of Physics, Pabna University of Science and Technology, Pabna-6600, Bangladesh.
*Correspondence: atik0707phy@gmail.com (Md. Atikur Rahman, Assistant Professor, Dept. of Physics, Pabna University of Science and Technology, Pabna, Bangladesh)

## ABSTRACT

$BaNiSn_3$-type superconductors $SrIrGe_3$, $SrPdGe_3$ and $SrPtGe_3$ have the critical temperature of 1.80 K, 1.49K and 1.0K respectively have been reported recently. Employing the first-principles method based on the density function theory, we have examined the physical properties including structural, elastic, electronic and optical phenomena of all these structures. For all the phases our optimized lattice parameters are well accord to the experimental lattice parameters. The positive elastic constants of these compounds revealed that these superconductors possess the mechanical stability in nature. The values of Pugh's ratio and Poisson's ratio ensured the brittle manner of these compounds and anisotropic behavior is ensured by the values of anisotropy factor. The soft nature of all compounds is confirmed by the bulk modulus analysis. The values of Vickers hardness indicate that the rigidity decreased in the order of $SrIrGe_3$>$SrPtGe_3$>$SrPdGe_3$. The overlapping of the conduction band and valence band at Fermi level indicates the zero band gaps and metallic nature of $SrIrGe_3$, $SrPdGe_3$ and $SrPtGe_3$. The chief contribution around the Fermi level arises from Ir-5d, Ge-4s, 4p states for $SrIrGe_3$ and Ge-4s, 4p states for $SrPdGe_3$ and Pt-5d, Ge-4s, 4p for $SrPtGe_3$ compound. The study of DOS, Mulliken atomic populations and charge density ensured the existing of complex bonding in $SrIrGe_3$, $SrPdGe_3$ and $SrPtGe_3$ with ionic, covalent and metallic characteristics. The analysis of the dielectric function also ensured the metallic behavior of all these compounds.

**Keywords:** $SrIrGe_3$, $SrPdGe_3$ and $SrPtGe_3$ superconductors, Chemical bonding, and Optical properties.

## 1. INTRODUCTION

The noncentrosymmetric superconductors have attracted much consideration having their unique superconducting properties caused by the Rashba-type antysymmetric spin-orbit coupling which leads to a mixing of the spin-singlet and spin-triplet states [1]. The investigations of specific conditions for superconductivity (SC) in non-centrosymmetric compounds were induced in 2004 by the discovery of heavy-fermion SC in $CePt_3Si$ with the superconducting critical temperature, Tc = 0.75 K [2]. Since the first heavy fermion noncentrosymmetric superconductor $CePt_3Si$ was discovered [2], a lot of similar systems have been found. In recent years, $BaNiSn_3$-type $LnTX_3$ compounds (Ln = lanthanide element, T = transition metal and X = Ge, Si) have been extensively investigated because of their interesting physical properties such as valance fluctuations [3-5] and

different magnetic properties [6-11]. Moreover, $CeIrGe_3$ [12], $CeIrSi_3$ [13-15] $CeCoGe_3$ [16, 17] and $CeRhSi_3$ [18, 19] with $BaNiSn_3$-type structure have been found to exhibit pressure induced superconductivity. This finding is very interesting because along the c-axis their structure lacks inversion symmetry. These Ce-based noncentrosymmetric superconductors (NCS) are placed close to a magnetic quantum critical point, making it difficult to show the effects of ASOC and inversion symmetry breaking on superconductivity.

In order to analysis the impact of inversion symmetry breaking on superconductivity, nonmagnetic Rashba-type NCS must be discovered and studied because the extra complications that originate from strong f-electron correlations can be prohibited. Among compounds adopting the tetragonal BaNiSn3-type structure [20], the phenomenon of superconductivity has been reported for $LaPdSi_3$ (Tc = 2.60-2.65 K [21, 22]), $LaRhSi_3$ (Tc = 2.16 K [22]), $LaPtSi_3$ (Tc = 1.52 K [23]), $BaPtSi_3$ (Tc = 2.25 K [24]), $CaPtSi_3$ (Tc = 2.3 K [25]), $CaIrSi_3$ (Tc = 3.3 K [26]), $SrPdGe_3$ (Tc = 1.49 K [27]), and $SrPtGe_3$ (Tc = 1.0 K [27]). Despite of the deficiency of centrosymmetry in the crystal structure, all these systems exhibit a typically BCS-like SC, except for CaIrSi3 [26] having a weakly anisotropic superconducting gap. The electronic properties of these $BaNiSn_3$-type NCS can affect their superconducting properties caused by electron-phonon interactions. In turn, in this family, pressure-inducted heavy-fermion SC has been detected in $CeCoGe_3$ (Tc = 0.7 [28]), $CeRhSi_3$ (Tc = 0.72 [29]), and $CeCoGe_3$ (Tc = 0.7 $CeIrGe_3$ (Tc = 1.6 K [30]).

In the current study, we therefore make a plan to investigate the physical properties including structural properties, elastic properties, electronic properties, optical properties of $SrIrGe_3$, $SrPdGe_3$ and $SrPtGe_3$ compounds. We have used the density functional theory (DFT) based on CASTEP computer program to discuss the detailed physical characteristics of these compounds. The remaining parts of this research work are organized as follows: the computation detail is given in second section then the result and discussion are given and finally the summary of our study is given.

## 2. THEORITICAL METHODS

The investigation of different properties of $SrMGe_3$ (where M= Ir, Pt, and Pd) compounds have been carried out using Cambridge Serial Total Energy Package (CASTEP) code based on the density functional theory (DFT) [31, 32]. The Ge-$4s^2 4p^2$, Sr-$4s^2 4p^6 5s^2$ and Ir-$5d^7 6s^2$; Ge-$4s^2 4p^2$, Sr-$4s^2 4p^6 5s^2$ and Pd-$4d^{10}$; Ge-$4s^2 4p^2$, Sr-$4s^2 4p^6 5s^2$ and Pt-$5d^9 6s^1$ are treated as the valance electrons in the case of $SrIrGe^3$, $SrPdGe^3$ and $SrPtGe^3$ respectively for pseudo atomic calculations. The wave functions are expanded using plane-wave cut-off energy 550eV with 10×11×13 grids for $SrIrGe_3$ and $SrPtGe_3$ compound and energy 500eV with 10×10×12 grids for $SrPdGe_3$ based on Monkhorst-Pack scheme [33] in the primitive cell. The Brodyden-Fletcher-Goldfarb-Shanno (BFGS) energy minimizing technique has been observed to optimize the crystal structure [34].

The parameters for the geometry optimization convergence criteria were imputed at $1.0 \times 10^{-5}$ eV/atom for the total energy, 0.03 eV/Å for maximum force, 0.05GPa for maximum stress and 0.001 Å for maximum displacement. The elastic stiffness constants are attained using the stress-strain method [35].

## 3. RESULTS AND DISCUSSION

**3.1 Structural Properties -** All the three noncentrosymmetric $SrMGe_3$ (M= Ir, Pt, and Pd) compounds investigated here belong to BaNiSn3-type tetragonal crystal structure with the space group I4/mmm (139). Each primitive cell unit cell contains one Sr atom at the 2a(0.00, 0.00, 0.00) position, one M atom at 2a(0.00, 0.00, ZT), one $Ge_1$ atom at 4b(0.00, 0.50, $ZGe_1$) and two $Ge_2$ atom at the 2a(0.00, 0.00, $ZGe_2$) sites. This three internal parameters (ZT, $ZGe_1$ and $ZGe_2$) and two lattice parameters (a and c) characterize the crystal structure of all these compounds. The calculated lattice parameters, tetragonal ratio, volume, bulk modulus and internal parameters are listed in **Table 1** for all the investigated NCS with the available experimental values. Here the slight deviation of the optimized lattice parameters

from the experimental values ensures the accuracy of our DFT based calculations. However in some cases we have observed that the optimized lattice parameters are slightly greater than the experimental values which happened due to the over estimation of the GGA based calculations.

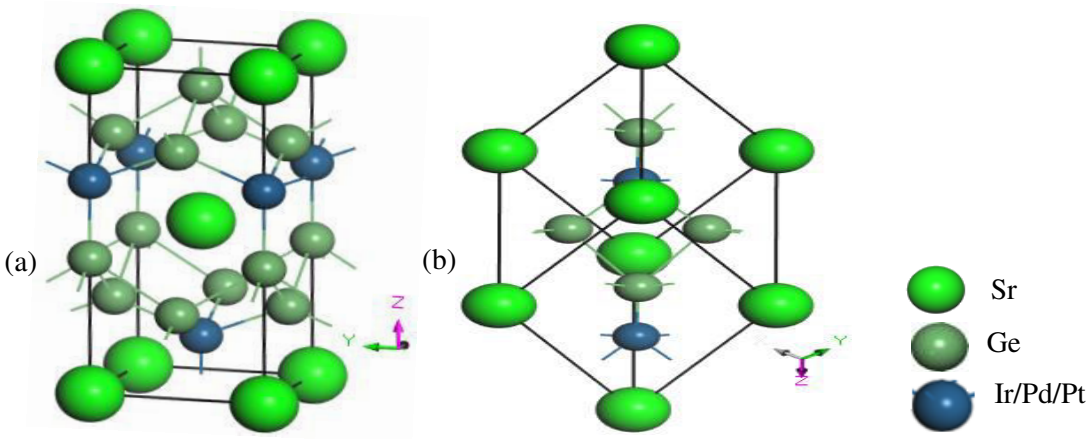


**Fig 1:** The crystal structures of $SrMGe_3$ (M=Ir, Pd and Pt); (a) Two dimensional conventional unit cell and (b) Three dimensional primitive unit cell.

**Table 1:** Structural parameters for $SrMGe_3$ (M=Ir, Pd and Pt) compounds and their comparison with the available experimental results.

| Material | *a*(Å) | *c*(Å) | *c**a* | *V*(Å$^3$) | *B*(GPa) | $Z_T$ | $Z_{Ge1}$ | $Z_{Ge2}$ | Remarks |
|---|---|---|---|---|---|---|---|---|---|
| | 4.508 | 10.190 | 2.261 | 207.082 | 82.776 | ---- | ---- | ---- | This work |
| **$SrIrGe_3$** | 4.465 | 10.091 | 2.260 | 201.176 | ---- | 0.649 | 0.254 | 0.412 | [36] |
| | 0.963 | 0.981 | 0.044 | 2.936 | ---- | ---- | ---- | ---- | Dev. (%) |
| | 4.495 | 10.360 | 2.304 | 209.324 | 71.854 | ---- | ---- | ---- | This work |
| **$SrPdGe_3$** | 4.462 | 10.274 | 2.303 | 204.550 | ---- | 0.642 | 0.253 | 0.399 | [36] |
| | 0.740 | 0.837 | 0.044 | 2.334 | ---- | ---- | ---- | ---- | Dev. (%) |
| | 4.468 | 10.503 | 2.350 | 209.672 | 78.288 | ---- | ---- | ---- | This work |
| **$SrPtGe_3$** | 4.478 | 10.137 | 2.264 | 203.272 | ---- | 0.645 | 0.257 | 0.401 | [36] |
| | 0.223 | 3.611 | 3.799 | 3.148 | ---- | ---- | ---- | ---- | Dev.(%) |

**3.2 Elastic constants and mechanical properties -** The elastic constants of any material are strongly correlated with the long-wavelength phonon spectrum; in this manner the elastic properties of super conducting material must be executed [37]. The important information about the dynamic features of crystalline materials is also provided by the elastic constants. The material's stability, ductility, brittleness, anisotropy, stiffness behavior and bonding nature in atom are obtained from the study of mechanical properties. According to the Hook's law, the elastic constants were carrying on from a linear fit of the evaluated stress-strain function [38]. The calculated elastic constants of $SrIrGe_3$, $SrPdGe_3$ and $SrPtGe_3$ superconductors are represent in **Table 2**. For tetragonal phase, the elastic constants need to content

the stability conditions known as the Born stability criteria [39].

$$C_{11} > 0;\ C_{33} > 0;\ C_{66} > 0;\ C_{44} > 0$$
$$C_{11} + C_{12} - 2C_{13} > 0;\ C_{11} - C_{12} > 0 \quad (1)$$
$$2(C_{11} + C_{12}) + 4C_{13} + C_{33} > 0$$

We have listed the observed elastic constants for $SrIrGe_3$, $SrPdGe_3$ and $SrPtGe_3$ superconductors in **Table 2**. From below **Table 2** we can see that the observed values are positive and gratified the above criteria. Hence we can say that the $SrIrGe_3$, $SrPdGe_3$ and $SrPtGe_3$ superconductors are mechanically stable in nature. It is seen that $C_{11}$ is significantly smaller than $C_{33}$, indicating that the chemical bonding strength in the (100) and (010) directions is significantly weaker than the bonding strength in the (001) direction. The value of $C_{44}$ is obviously smaller than $C_{66}$, which demonstrates that it is easier for shear deformation to occur along the (001) direction in comparison with the (010) direction.

**Table 2:** The calculated single independent elastic constants $C_{ij}$ (in Gpa) of $SrIrGe_3$, $SrPdGe_3$ and $SrPtGe_3$ superconductor.

| | Elastic Constants | | | | | | |
|---|---|---|---|---|---|---|---|
| **Compounds** | $C_{11}$ | $C_{12}$ | $C_{13}$ | $C_{33}$ | $C_{44}$ | $C_{66}$ | Ref. |
| **$SrIrGe_3$** | 147.521 | 39.899 | 54.994 | 151.513 | 38.879 | 40.333 | This study |
| **$SrPdGe_3$** | 93.572 | 69.128 | 53.356 | 107.874 | 37.101 | 34.268 | This study |
| **$SrPtGe_3$** | 115.233 | 60.503 | 57.982 | 121.263 | 42.270 | 36.231 | This study |
| **$LaIrSi_3$** | 211.95 | 67.98 | 108.56 | 217.21 | 41.41 | 62.57 | [40] |

According to the Voigt-Reuss-Hill (VRH) average schemes [41], the shear modulus ($G$), the bulk modulus ($B$), Poisson ratio ($v$) and Young's modulus ($E$) can be calculated for the tetragonal system. The bulk and shear moduli given as follows:

$$B_V = \frac{2C_{11}+2C_{12}+C_{33}+4C_{13}}{9} \quad (2)$$

$$B_R = \frac{C^2}{M} \quad (3)$$

$$G_V = \frac{M+3C_{11}-3C_{12}+12C_{44}+6C_{66}}{30} \quad (4)$$

$$G_R = 15\left[\frac{18B_V}{C^2} + \frac{6}{(C_{11}-C_{12})} + \frac{6}{C_{44}} + \frac{3}{C_{66}}\right]^{-1} \quad (5)$$

Where $C^2 = (C_{11} + C_{12})C_{33} - 2C_{13}^2$

And $M = C_{11} + C_{12} + 2C_{33} - 4C_{13}$

$$B = \frac{B_V+B_R}{2} \quad (6)$$

$$G = \frac{G_V+G_R}{2} \quad (7)$$

We have calculated the Poisson's ratio ($v$) and the Young's modulus ($E$) using the following equations,

$$E = \frac{9GB}{3B+G} \quad (8)$$

$$v = \frac{3B-2G}{2(3B+G)} \quad (9)$$

The calculated values of Bulk modulus $B$, Shear modulus $G$, Young modulus $E$, $B/G$ and $v$ for the compounds $SrMGe_3$ (M = Ir, Pd and Pt) are listed in **Table 3**. It has been seen from **Table 3** that the values of B of $SrIrGe_3$, $SrPdGe_3$ and $SrPtGe_3$ are less than 100 GPa [42] indicating that these are relatively soft materials. The stiffness properties of a compound can be described by Young modulus $E$. The larger value of $E$ signifies the more stiffness of a compound [43]. These compounds also show the larger bulk modulus $B$ than the shear modulus $G$ expressing the limitation of mechanical stability for these compounds by $G$ [44].

Generally, it is extremely helpful to predict the type of bonding force which makes a solid to reveal ductility or brittleness behavior. The shear modulus $G$ is denoted by the resistance to plastic deformation and bulk modulus $B$ is defined by the resistance to fracture so that the flexibility of a material is observed by the well-known ratio $B/G$ called as Pough' ratio [43].

**Table 3:** Calculated polycrystalline bulk modulus *B* (GPa), shear modulus *G* (GPa), Young's modulus *E* (GPa), *B/G* values, Poisson's ratio *v*, elastic anisotropy index $A^{U}$ and Vickers hardness $H_v$ (GPa) of $SrMGe_3$ (M = Ir, Pd and Pt).

| Polycrystalline Elastic Properties | | | | | | | |
|---|---|---|---|---|---|---|---|
| **Compounds** | ***B*** | ***G*** | ***E*** | ***B/G*** | ***v*** | $A^U$ | $H_V$ |
| **$SrIrGe_3$** | 82.776 | 43.051 | 110.069 | 1.923 | 0.278 | 0.0846 | 5.409 |
| **$SrPdGe_3$** | 71.854 | 27.241 | 72.554 | 2.638 | 0.332 | 0.9655 | 1.444 |
| **$SrPtGe_3$** | 78.288 | 35.321 | 92.111 | 2.222 | 0.304 | 0.149 | 3.342 |

The ductile compound processes the larger value of $B/G\ (> 1.75)$ else the compound will be brittle. The lower value of Poisson' ratio $(\nu < 0.26)$ shows the brittleness properties of a compound and for any other values the compound will be ductile. According to these conditions $SrIrGe_3$, $SrPdGe_3$ and $SrPtGe_3$ process the brittleness manner. The universal anisotropy index $A^{U}$ can be evaluated by using the following equation [45]:

$$A^U = \frac{5G_V}{G_R} + \frac{B_V}{B_R} - 6 \qquad (10)$$

If $A^{U} = 0$ the crystal is entirely isotropic and any deviation from this value represent the degree of anisotropy in the crystal. According to the values of $A^{U}$ exhibited in **Table 3** our studied compounds show anisotropic behavior. It is also obvious that $SrPdGe_3$ is more anisotropic among them. The Vickers hardness which is also an important mechanical property of a material is obtained by the following equation proposed by *Chen et al.* [46].

$$H_V = 2(K^2G)^{0.585} - 3 \qquad (11)$$

In **Table 3** the values of Vickers hardness are tabulated. It is evident from Table 3 that $SrIrGe_3$, $SrPdGe_3$ and $SrPtGe_3$ are relatively soft materials which are contradicted by softness/hardness characteristics presented by the bulk modulus *B*.

**3.3 Electronic Properties and Chemical Bonding -** The electronic band structure, partial density of states (PDOS) and total density of states (TDOS) of $SrIrGe_3$, $SrPdGe_3$ and $SrPtGe_3$ have been studied and discussed to gain the deep insights into the electronic properties of these superconductors. The Fermi level between conduction band and valance band is indicated in diagram along with the range of total band structure. The electronic band structure diagrams for these compounds are depictured in **Fig 2**. In these diagrams we can see that the valance band and conduction band are overlapped at Fermi level ($E_F$) and there is no band gap appeared at $E_F$. Since there is no band gap it can be implies that these compounds under study shows metallic behavior and the metallic nature of $SrIrGe_3$, $SrPdGe_3$ and $SrPtGe_3$ implies that these compound might be superconductor [47]. The densities of states (partial and total) of $SrIrGe_3$, $SrPdGe_3$ and $SrPtGe_3$ compounds are plotted on **Fig 3**. The lower valance bands for $SrIrGe_3$ (-17.59eV to -16.38eV) and for $SrPdGe_3$ (-18.73eV to -17.57eV) are consists from Sr-4p state which is dominant for these compounds and for SrPtGe3 (-18.07eV to -16.83eV) consist from Sr-4s, 5s state. The middle valance band for $SrIrGe_3$ (to be found at -11.64eV to -6.49eV), for $SrPdGe_3$ (to be found at -12.48eV to -7.13eV) and for $SrPtGe_3$ (to be found at 12.20eV to 6.68eV) are made up from Ge-4s state.

For $SrIrGe_3$ the upper valance band (to be found at -5.72eV to 0eV) is mainly originates from Ir-5d, Ge-4p states and Pd-4d, Ge-4p for $SrPdGe_3$ (to be found at -6.24eV to 0eV).For $SrPtGe_3$ the upper valance band (to be found at -6.36eV to 0eV) is mainly originates from Pt-5d and Ge-4p states. The contribution of Ge-4p states is dominant for all compounds. The conduction band mainly contributed from Ir-5d and Ge-4s, 4p states in case of $SrIrGe_3$ and Ge-4s, 4p state for $SrPdGe_3$ and $SrPtGe_3$ whereas Ge-4s, 4p orbital is dominant for all compounds. At the Fermi level mainly contribution comes from Ir-5d, Ge-4s, 4p states for $SrIrGe_3$ and Ge-4s, 4p states for $SrPdGe_3$ and Pt-5d, Ge-4s,4p for $SrPtGe_3$ compounds.

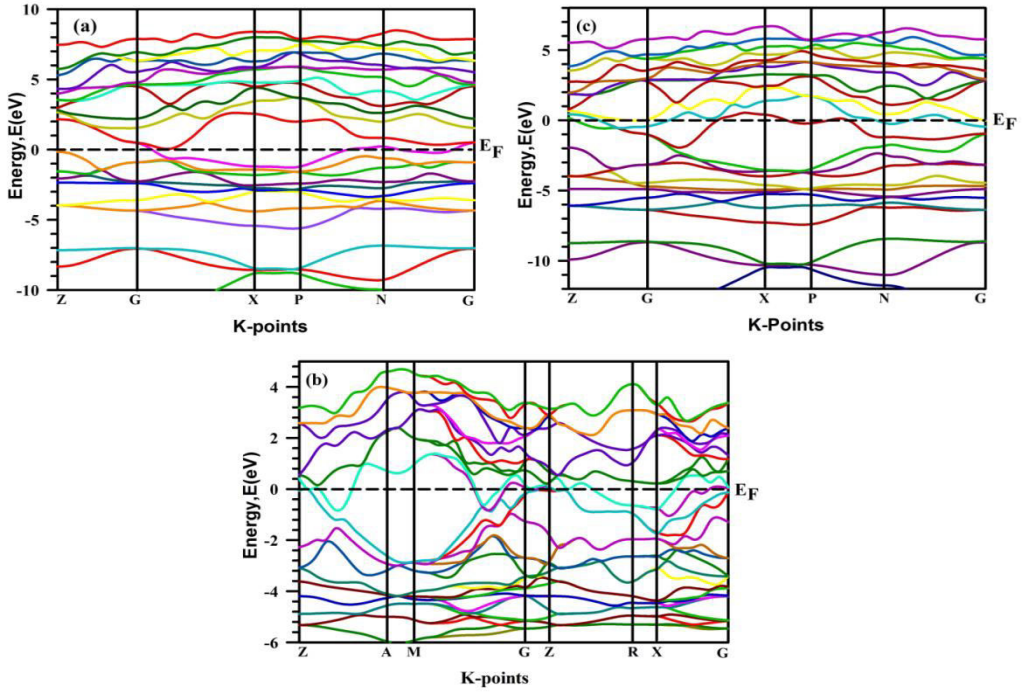


**Fig 2:** The electronic band structure of (a) $SrIrGe_3$, (b) $SrPdGe_3$ and (c) $SrPtGe_3$ ternary intermetallics along high symmetry direction in the Brillouin zones.

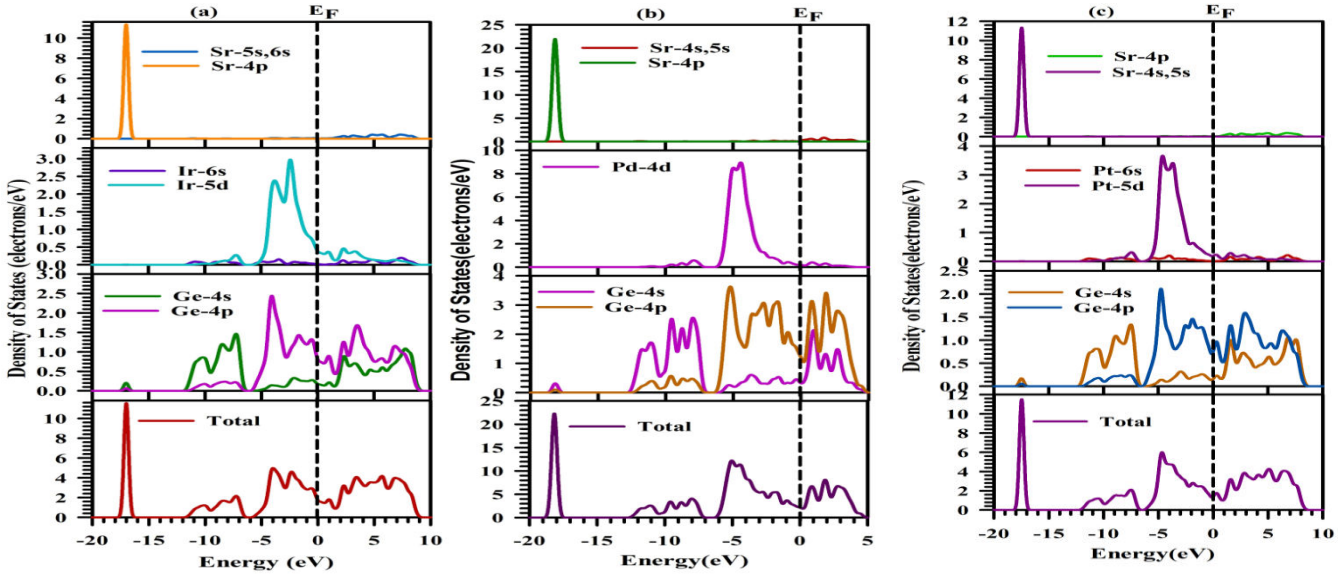


**Fig 3:** Total and partial density of states for (a) $SrIrGe_3$, (b) $SrPdGe_3$ and (c) $SrPtGe_3$.

The calculated values of density of states at the Fermi level are 1.96eV states $eV^{-1}$ $fu^{-1}$, 2.39eV states $eV^{-1}$ $fu^{-1}$ and 1.52 states $eV^{-1}$ $fu^{-1}$ for $SrIrGe_3$, $SrPdGe_3$ and $SrPtGe_3$ respectively. Which type of bond exists in these compounds is clearly known by study of Mulliken atomic population. Here we have study The Mulliken atomic population of these compounds and presented in **Table 4**. From **Table 4** we have seen that Sr and Ge atoms have positive charge while Ir contains negative charge for $SrIrGe_3$ compound which indicates the charge transferring from Sr and Ge atoms to Ir atom. Similarly the charge transfers from Sr and Ge atoms to Pd atom in case of $SrPdGe_3$ compound and charge transferring from Sr and Ge atoms to Pt atom in case of $SrPtGe_3$ compound. The zero value of band population exhibits a perfect ionic bond and greater than zero initiative the increase of covalence bond [48].

**Table 4:** Mulliken atomic populations of $SrIrGe_3$, $SrPdGe_3$ and $SrPtGe_3$ compounds.

| Compounds | Species | S | P | D | Total | Charge | Bond | Population | Lengths |
|---|---|---|---|---|---|---|---|---|---|
| | Sr | 2.26 | 5.97 | 0.96 | 9.19 | 0.81 | | | |
| **$SrIrGe_3$** | Ir | 0.73 | 1.04 | 8.02 | 9.79 | -0.79 | Ge-Ir | 0.31 | 2.483 |
| | Ge | 1.38 | 2.50 | 0.00 | 3.88 | 0.12 | Ge-Ge | -5.80 | 2.784 |
| | Sr | 2.24 | 5.97 | 0.91 | 9.12 | 0.88 | | | |
| **$SrPdGe_3$** | Pd | 0.73 | 1.21 | 9.37 | 11.30 | -1.30 | Ge-Pd | 0.21 | 2.499 |
| | Ge | 1.31 | 2.42 | 0.00 | 3.73 | 0.27 | Ge-Ge | -3.34 | 2.717 |
| | Sr | 2.23 | 5.97 | 0.92 | 9.12 | 0.88 | | | |
| **$SrPtGe_3$** | Pt | 0.89 | 1.18 | 8.96 | 11.03 | -1.03 | Ge-Pt | -0.81 | 2.507 |
| | Ge | 1.37 | 2.44 | 0.00 | 3.81 | 0.19 | | | |

The values of population of Ge-Ir, Ge-Pd are greater than zero, which indicates that these bonds are covalent. The values of population of Ge-Ge, Ge-Pt are negative and indicating the ionic character. These results accrue with the result of density of states (DOS) analysis. In order to get clear insight into the bonding the total charge density map for $SrIrGe_3$, $SrPdGe_3$ and $SrPtGe_3$ compounds are shown in **Fig 4**. The blue and red colors indicate the low and high electron densities respectively. We observe a clear overlapping of charge density distribution between the nearest Ge, Ir and Ge, Pd atoms indicating the covalent nature of Ge-Ir for $SrIrGe_3$ and Ge-Pd bonds for $SrPdGe_3$ compound. These results show a good consent with the DOS analysis. There is no overlapping of electron (charge) distribution among Sr atoms indicating the ionic feature Sr-Sr bonds of SrIrGe3 and SrPdGe3 compounds. For SrPtGe3 compound the Sr and Ge atoms shows the covalent nature and Pt shows the ionic nature. The ionic character is consequence of the metallic nature [49] viewing the metallic behavior of Sr-Sr, and Pt-Pt bonds.

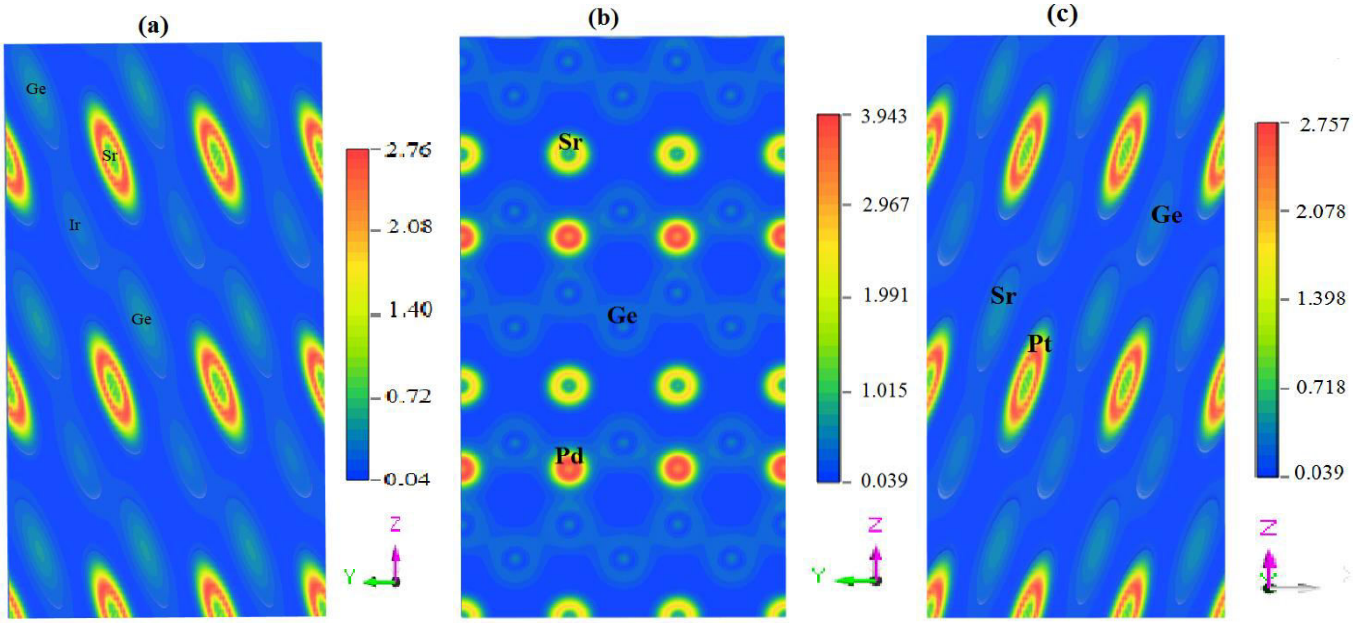


**Fig 4:** Total charge density of (a) $SrIrGe_3$, (b) $SrPdGe_3$ and (c) $SrPtGe_3$ compounds.

Hence from the overall detailed study of DOS, Mulliken atomic population and total charge density of SrMGe3 (M=Ir, Pd, Pt) superconductors we can conclude that all compounds have ionic, covalent and metallic bonds which is the common characteristics of $BaNiSn_3$ structured compounds.

**3.4 Optical properties -** Using the frequency dependent dielectric function $\varepsilon(\omega) = \varepsilon_1(\omega)+i\varepsilon_2(\omega)$, the optical properties of $SrIrGe_3$, $SrPdGe_3$ and $SrPtGe_3$ superconductors have been studied. The investigation of the optical function of solids provides excessive information of the electronic properties. From the momentum matrix elements between the unfilled and filled electronic states the imaginary part, $\varepsilon_2(\omega)$ of dielectric function can be obtain [50]. This is express by the following function,

$$\varepsilon_2(\omega) = \frac{2e^2\pi}{\Omega\varepsilon_0}\sum_{k,v,c}\left|\psi_k^c\right|u.r\left|\psi_k^v\right|^2\delta(E_k^c - E_k^v - \hbar\omega) \qquad (12)$$

Where $u$ represent the polarization of the incident electric field, ω as the frequency of light, **Ω** represent the until cell volume, , e is define as the charge of electron, $\left|\psi_k^c\right|$ and $\left|\psi_k^v\right|$ represent respectively the conduction band wave function and valance band wave function at *K*. By using Kramers-Kronig transformation the real part $\varepsilon_1(\omega)$ can be obtained from the value of $\varepsilon_2(\omega)$. The optical properties such as absorption spectrum, loss function, conductivity, dielectric function, reflectivity and refractive index are evaluated by eqs (49)-(54) in ref [51].

The absorption spectra offer useful information about the maximum solar energy exchange efficiency and it show how far light of specific wavelength is passes through a material before being absorbed. The absorption spectra of SrMGe3 (M=Ir, Pd, Pt) are shown in **Fig 5(a)**. **Fig 5(a)** shows the absorption coefficients of all the phases which begin at 0 eV due to their metallic nature. It has been seen that the nature of absorption curves are almost same for these compounds. Two strong peaks (absorption) are found in the visible and ultraviolet regions for all phases at different energy ranges. These peaks are weak in the visible region but continuously increase in the ultraviolet region and reach maximum value at 9.00 eV. According to this outcome we can say that $SrIrGe_3$, $SrPdGe_3$ and $SrPtGe_3$ compounds are promising for absorbing materials in the UV region. All the compounds show rather good absorption coefficient in the 9.0 eV to 23.85 eV regions. The spectra of reflectivity of $SrIrGe_3$, $SrPdGe_3$ and $SrPtGe_3$ are shown in **Fig 5(b)**. Reflectivity is a function of incident light energy and is a measure of the ability of a surface to reflect radiation incident on it. It is attained by the ratio of the energy of the wave reflected from a surface to the energy of the wave incident on the surface [52]. From **Fig 5(b)** we can see that the reflectivity starts from the value of 0.60 for $SrIrGe_3$, 0.98 for $SrPdGe_3$ (it is also the maximum value) and 0.59 for $SrPtGe_3$ with zero photon energy. The maximum value of reflectivity appears at 12.36 eV energy is 0.69 for $SrIrGe_3$ compound, at 13.45 eV energy is 0.69 for $SrPtGe_3$ compound. It is also evident that all phases can be used as excellent coating materials in the energy range 1.5eV to 14.48 eV.

The reflectivity of these compounds is much higher in the ultraviolet and IR regions. Therefore all the compounds, with roughly similar reflectivity spectra, show good promise as good coating materials in the ultraviolet and infrared regions. The conductivity spectrum of $SrIrGe_3$, $SrPdGe_3$ and $SrPtGe_3$ are shown in **Fig 5(c)**. The conductivity is an optoelectronic phenomenon in which electrical conductivity of a material rises as a result of absorbing of photons. It helps us to mark out the material will be semiconductor, conductor or superconductor. The investigated conductivity spectra with photon energy of $SrMGe_3$ (M=Ir, Pd, Pt) are shown in **Fig 5(c)**. The photoconductivity starts with zero photon energy due to the reason that the materials have no band gap which is apparent from band structure signifying the metallic behaviors of these phases. The photoconductivity is maxima at 5.18 eV for SrIrGe3 and 2.84 eV for $SrPdGe_3$ and $SrPtGe_3$ compound. No photoconductivity occurs above 26.19 eV.

The energy loss function is defined as the energy loss of a fast electron when it traverses in the material [53]. The frequency at which maximum energy loss happened is known as the Bulk plasma frequency $\omega_p$ of the material which emerges at $\varepsilon_1(\omega) = 0$ and $\varepsilon_2(\omega)$ is less than one [54, 55]. The energy loss spectra for all these three compounds under investigation are plotted in **Fig 5(d)**. The loss function is maxima at 14.90 eV for $SrIrGe_3$ and $SrPtGe_3$ compound and 12.44 eV for $SrPdGe_3$ compound. These materials become transparent when the plasma frequency is lower than that of incident frequency.

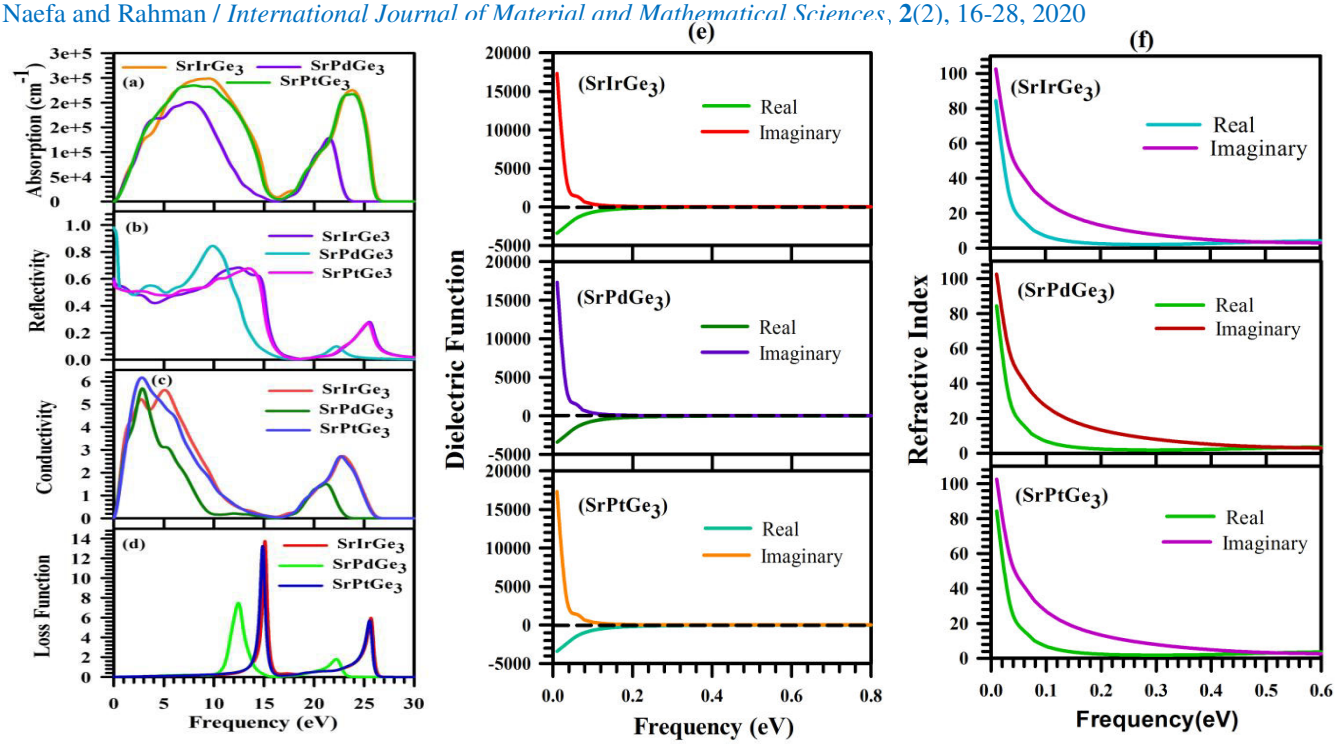


**Fig 5:** The optical functions (a) Absorption, (b) Reflectivity, (c) Conductivity, and (d) Loss function of $SrIrGe_3$, $SrPdGe_3$ and $SrPtGe_3$. (e) Dielectric function of $SrIrGe_3$, $SrPdGe_3$ and $SrPtGe_3$ (f) Refractive index of $SrIrGe_3$, $SrPdGe_3$ and $SrPtGe_3$.

Dielectric function is a crucial factor to know the energy loss and polarizability of a material, while electromagnetic wave passes through it. The real and imaginary parts of dielectric function are shown in **Fig 5(e)** for $SrIrGe_3$, $SrPdGe_3$ and $SrPtGe_3$ compounds. It is obvious from the study of chemical bonding and electronic structure that these compounds show metallic behavior in nature. Hence it is necessary to include the Drude term to the dielectric function [53, 56, and 57].

The unscreened plasma frequency 3 eV and damping (relaxation energy) 0.05 eV have been used in the Drude term. Despite some variation in heights and position of peaks, the overall features of our calculated optical spectra of $SrIrGe_3$, $SrPdGe_3$ and $SrPtGe_3$ are almost similar. It has been observed that for all the phases the real part $\varepsilon_1(\omega)$ of the dielectric function became zero at around 0.16 eV, which corresponds to the energy at which the absorption coefficients nearly zero (**Fig 5a**), reflectivity shows a sharp drop (**Fig 5b**) and the conductivity (**Fig 5c**) increases sharply. The large negative value $\varepsilon_1(\omega)$ of dielectric constant exhibit the Drude-like behaviors which is common feature for metallic system From **Fig 5(e)** we have observed that real part of the dielectric function comes to zero from below and the imaginary part of the dielectric function comes to zero from above which also ensure the metallic nature of these compounds.

When light is entered into a material then it is refracted or bent. So how much light is refracted or bent when it traversing through a material, this quantity is measured by a dimensionless parameter called the refractive index [58]. The idea of refractive index of an optical material is very effective for its use in optical tools such as waveguides, photonic crystals, etc.

The refractive indices in terms of real and imaginary of $SrIrGe_3$, $SrPdGe_3$ and $SrPtGe_3$ are displayed in **Fig 5(f)**. The imaginary part describes the amount of absorption loss and the real part signifies the phase velocity of electromagnetic wave when propagates throughout the material. For all superconductors the static refractive index n (0) is found to have the value 104.

## 4. COCLUSION

In this research work, we have performed the detailed physical properties including structural, elastic, electronic, chemical bonding and optical properties of $SrIrGe_3$, $SrPdGe_3$ and $SrPtGe_3$ by using CASTEP code based on the density functional theory. The optimize lattice parameters have a slight variation from available experimental data for all compounds. The studies of Pugh's ratio values revealed that all compounds are brittle in nature and the value of Poisson's ratio suggests that central force exists in these compounds. The bulk modulus indicated the soft behavior of $SrIrGe_3$, $SrPdGe_3$ and $SrPtGe_3$ compounds. The study of elastic constant ensured that all compounds are stable in nature and show anisotropic manner. The band structures and density of states (DOS) revealed the metallic nature of these phases. The chemical bonding analysis ensured the existing of covalent, ionic and metallic bonds in these compounds. The reflection spectra of all the compounds showed that these have the potential to be used as coating material to avoid solar heating up to ~8 eV. The large negative values of real part of the dielectric function revealed the metallic nature of all these compounds. The conductivity spectrum and the absorption coefficient are started from zero energy which also indicated the metallic features of all the compounds.

## 5. ACKNOWLEDGEMENT

We would like to thank Department of Physics, Pabna University of Science and Technology, Bangladesh for the condensed matter lab support.

## 6. CONFLICTS OF INTEREST

We have no conflict of interest about this article.

## 7. REFERENCES

1. Gor'kov, L.P. and Rashba, E.I. (2001). Superconducting 2D system with lifted spin degeneracy: mixed singlet-triplet state. *Physical Review Letters*, **87**(3), p.037004. https://doi.org/10.1103/PhysRevLett.87.037004
2. Bauer, E., Hilscher, G., Michor, H., and Rogl, P. (2004). Heavy fermion superconductivity and magnetic order in noncentrosymmetric $CePt_3Si$. *Physical Review Letters*, **92**(2), p.027003.
3. Seropegin, Y.D., Shapiev, B.I., and Bodak, O.I. (1999). Isothermal cross-section of the Ce-Ru-Si phase diagram at 600 C. *J. of alloys and compounds*, **288**(1-2), pp.147-150.
4. Kawai, T., Muranaka, H., and Flouquet, J. (2008). Magnetic and superconducting properties of $CeTX_3$ (T: transition metal and X: Si and Ge) with non-centrosymmetric crystal structure. *J. of the Physical Society of Japan*, **77**(6), pp.064716-064716.
5. Smidman, M., Adroja, D.T., and Balakrishnan, G. (2015). Evidence for a hybridization gap in noncentrosymmetric $CeRuSi_3$. *Physical Review B*, **91**(6), p.064419. https://doi.org/10.1103/PhysRevB.91.064419
6. Kumar, N., Dhar, S.K., and Manfrinetti, P. (2010). Magnetic properties of $EuPtSi_3$ single crystals. *Physical Review B*, **81**(14), p.144414.
7. Kumar, N., Das, P.K., Kulkarni, R., and Bonville, P. (2011). Antiferromagnetic ordering in $EuPtGe_3$. *Journal of Physics: Condensed Matter*, **24**(3), p.036005.
8. Kaczorowski, D., Belan, B. and Gladyshevskii, R. (2012). Magnetic and electrical properties of $EuPdGe_3$. *Solid state communications*, **152**(10), pp.839-841. https://doi.org/10.1016/j.ssc.2012.02.022
9. Goetsch, R.J., Anand, V.K. and Johnston, D.C. (2013). Anti ferromagnetism in $EuNiGe_3$. *Physical Review B*, **87**(6), p.064406.
10. Bednarchuk, O., Gągor, A. and Kaczorowski, D. (2015). Synthesis, crystal structure and physical properties of $EuTGe_3$ (T= Co, Ni, Rh, Pd, Ir, Pt) single crystals. *J. of Alloys and Compounds*, **622**, pp.432-439.
11. Maurya, A., Bonville, P., and Dhar, S.K. (2016). Magnetic properties and complex magnetic phase diagram in non-centrosymmetric $EuRhGe_3$ and $EuIrGe_3$ single crystals. *J. of Magnetism and Magnetic Materials*, **401**, pp.823-831. https://doi.org/10.1016/j.jmmm.2015.10.134

12. Honda, F., Bonalde, I., and Ōnuki, Y. (2010). Pressure-induced superconductivity and large upper critical field in the noncentrosymmetric antiferromagnet $CeIrGe_3$. *Physical Review B*, **81**(14), p.140507.
13. Mukuda, H., Fujii, T., Ohara, T., Harada, A., and Onuki, Y. (2008). Enhancement of superconducting transition temperature due to the strong antiferromagnetic spin fluctuations in the noncentrosymmetric heavy-Fermion superconductor $CeIrSi_3$: A Si29 NMR study under pressure. *Physical review letters*, **100**(10), p.107003.
14. Tada, Y., Kawakami, N. and Fujimoto, S. (2010). Spin fluctuations and super conductivity in noncentrosymmetric heavy fermion systems $CeRhSi_3$ and $CeIrSi_3$. *Physical Review B*, **81**(10), p.104506. https://doi.org/10.1103/PhysRevB.81.104506
15. Szlawska, M. and Kaczorowski, D. (2011). Antiferromagnetic order and Kondo effect in single-crystalline $Ce_2IrSi_3$.*Physical Review B*, **84**(9), p.094430.
16. Settai, R., Sugitani, I., Okuda, Y., Thamizhavel, and Harima, H. (2007). Pressure-induced superconductivity in $CeCoGe_3$ without inversion symmetry. *J. of magnetism and magnetic materials*, **310**(2), pp.844-846.
17. Smidman, M., Adroja, D.T., Chapon, L.C., and Krishnamurthy, V.V. (2013). Neutron scattering and muon spin relaxation measurements of the noncentrosymmetric antiferromagnet $CeCoGe_3$. *Physical Review B*, **88**(13), p.134416.
18. Kimura, N., Ito, K., Saitoh, K., Umeda, Y., Aoki, H. and Terashima, T. (2005). Pressure-induced superconductivity in noncentro-symmetric heavy fermion $CeRhSi_3$. *Physical review letters*, **95**(24), p.247004. https://doi.org/10.1103/physrevlett.95.247004
19. Egetenmeyer, N., Gavilano, J.L., Maisuradze, A., Gerber, S., and Khasanov, R. (2012). Direct observation of the quantum critical point in heavy fermion $CeRhSi_3$. *Physical review letters*, **108**(17), p.177204.
20. Dörrscheidt, W. and Schäfer, H. (1978). Die struktur des $BaPtSn_3$, $BaNiSn_3$ und $SrNiSn_3$ und ihre verwandtschaft zum ThCr2Si2-strukturtyp. *Journal of the Less Common Metals*, **58**(2), pp.209-216. https://doi.org/10.1016/0022-5088(78)90202-3
21. Kitagawa, J., Muro, Y., Takeda, N., ISHIKAWA, M., Yamamoto, H., Oguro, I. and Ishikawa, M. (1997). *Journal of the Physical Society of Japan*, **66**(7), pp.2163-2174.
22. Anand, V.K., Hillier, A.D., Adroja, D.T., Strydom, A.M., and Rainford, B.D. (2011). Specific heat and μ SR study on the noncentrosymmetric superconductor $LaRhSi_3$. *Physical Review B*, **83**(6), p.064522.
23. Smidman, M., Hillier, A.D., Adroja, D.T., Lees, M.R., and Balakrishnan, G. (2014). Investigations of the superconducting states of noncentrosymmetric $LaPdSi_3$ and $LaPtSi_3$. *Physical Review B*, **89**(9), p.094509.
24. Bauer, E., Khan, R.T., Michor, H., and Wolf, W. (2009). $BaPtSi_3$: A noncentrosymmetric BCS like superconductor. *Physical Review B*, **80**(6), p.064504. https://doi.org/10.1103/PhysRevB.80.064504
25. Eguchi, G., Peets, D.C., Kriener, M., Maeno, Y., and Sawa, H. (2011). Crystallographic and superconducting properties of the fully gapped noncentrosymmetric 5 d-electron super conductors $CaMSi_3$ (M= Ir, Pt). *Physical Review B*, **83**(2), p.024512.
26. Eguchi, G., Wadati, H., and Maeno, Y. (2012). Large spin-orbit splitting and weakly anisotropic superconductivity revealed with single crystalline noncentrosymmetric $CaIrSi_3$. *Physical Review B*, **86**(18), p.184510.
27. Miliyanchuk, K., Kneidinger, F., Michor, H. and Bauer, E. (2011). Platinum metal silicides and germanides: superconductivity in non-centrosymmetric intermetallics. In *Journal of Physics: Conference Series*, **273**(1), p. 012078).
28. Settai, R., Sugitani, I., Okuda, Y., and Harima, H. (2007). Pressure-induced superconductivity in $CeCoGe_3$ without inversion symmetry.

*Journal of magnetism and magnetic materials*, **310**(2), pp.844-846. https://doi.org/10.1016/j.jmmm.2006.10.717

29. Kimura, N., Ito, K., Saitoh, K., Umeda, Y., Aoki, H. and Terashima, T. (2005). Pressure induced super conductivity in noncentro-symmetric heavy-fermion $CeRhSi_3$. *Physical review letters*, **95**(24), p.247004.
30. Honda, F., Bonalde, I., Yoshiuchi, S., Hirose, Y., and Ōnuki, Y. (2010). Pressure-induced superconductivity in non-centrosymmetric compound $CeIrGe_3$. *Physica C: Super conductivity and its applications*, **470**, pp.S543-S544.
31. Clark, S.J., Segall, M.D., Pickard, C.J., Hasnip, P.J., and Payne, M.C. (2005). First principles methods using CASTEP. *Zeitschrift für Kristallographie-Crystalline Materials*, **220**(5/6), pp.567-570.
32. Materials Studio CASTEP manual_Accelrys, (2010). 261–262. http://www.tcm.phy.cam.ac.uk/castep/documentation/WebHelp/CASTEP.html
33. Monkhorst, H.J. and Pack, J.D. (1976). Special points for Brillouin zone integrations. *Physical review B*, **13**(12), p.5188.
34. Pfrommer, B.G., Côté, M., Louie, S.G. and Cohen, M.L. (1997). Relaxation of crystals with the quasi-Newton method. *Journal of Computational Physics*, **131**(1), pp.233-240.
35. Kang, J., Lee, E.C. and Chang, K.J. (2003). First-principles study of the structural phase transformation of hafnia under pressure. *Physical Review B*, **68**(5), p.054106.
36. Fujii, H. and Sato, A. (2010). BaNiSn3-type ternary germanides $SrMGe_3$ (M= Ir; Pd and Pt). *J. of alloys and compounds*, **508**(2), pp.338-341. https://doi.org/10.1016/j.jallcom.2010.08.150
37. Kang, J., Lee, E.C. and Chang, K.J. (2003). First-principles study of the structural phase transformation of hafnia under pressure. *Physical Review B*, **68**(5), p.054106.
38. Ma, Y., Oganov, A.R. and Xie, Y. (2008). High-pressure structures of lithium, potassium, and rubidium predicted by an ab initio evolutionary algorithm. *Physical Review B*, **78**(1), p.014102.
39. Xiao, H.Y., Jiang, X.D., Duan, G., Gao, F., Zu, X.T. and Weber, W.J. (2010). First-principles calculations of pressure-induced phase transformation in AlN and GaN. *Computational materials science*, **48**(4), pp.768-772.
40. Uzunok, H.Y., Tütüncü, H.M., Srivastava, G.P., Ipsara, E. and Başoğlu, A. (2017). The effect of spin orbit interaction on the physical properties of $LaTSi_3$ (T= Ir, Pd, and Rh): First principles calculations. *Journal of Applied Physics*, **121**(19), p.193904. https://doi.org/10.1063/1.4983770
41. Hill, R. (1952). The elastic behaviour of a crystalline aggregate. *Proceedings of the Physical Society. Section A*, **65**(5), p.349.
42. ChaozhuShu, J.L. (2015). Shuangjie and Wenge Yang. *Journal of Superconductivity and Novel Magnetism,* **28**(11), pp.3235-3241.
43. Pugh, S.F. (1954). XCII. Relations between the elastic moduli and the plastic properties of polycrystalline pure metals. *The London, Edinburgh, and Dublin Philosophical Magazine and Journal of Science*, **45**(367), pp.823-843.
44. Shein, I.R. (2011). Stability, structural, elastic, and electronic properties of polymorphs of the superconducting disilicide $YIr_2Si_2$. *Physica B: Condensed Matter*, **406**(19), pp.3525-3530.
45. Ranganathan, S.I. and Ostoja-Starzewski, M. (2008). Universal elastic anisotropy index. *Physical Review Letters*, **101**(5), p.055504. https://doi.org/10.1103/PhysRevLett.101.055504
46. Chen, X.Q., Niu, H., Li, D. and Li, Y. (2011). Modeling hardness of polycrystalline materials and bulk metallic glasses. *Intermetallics*, **19**(9), pp.1275-1281.
47. Rahaman, M.Z. and Rahman, M.A. (2016). Novel Laves phase superconductor $NbBe_2$: A theoretical investigation. *Computational Condensed Matter*, **8**, pp.7-13.
48. Segall, M.D., Shah, R., Pickard, C.J. and Payne, M.C. (1996). Population analysis of

plane-wave electronic structure calculations of bulk materials. *Physical Review B*, **54**(23), p.16317.

49. Yildirim, T. (2009). Strong coupling of the Fe-spin state and the As-As hybridization in iron-pnictide superconductors from first-principle calculations. *Physical Review Letters*, **102**(3), p.037003. https://doi.org/10.1103/PhysRevLett.102.037003
50. Segall, M.D., Lindan, P.J., Probert, M.A., and Payne, M.C. (2002). First principles simulation: ideas, illustrations and the CASTEP code. *Journal of Physics: Condensed Matter*, **14**(11), p.2717.
51. Materials Studio CASTEP manual © Accelrys (2010). http://www.tcm.phy.cam.ac.uk/castep/documentation/WebHelp/CASTEP.html.
52. Roknuzzaman, M., Hadi, M.A., Abden, M.J., Nasir, M.T., Islam, A.K.M.A., Ali, M.S., Ostrikov, K. and Naqib, S.H. (2016). Physical properties of predicted $Ti_2CdN$ versus existing $Ti_2CdC$ MAX phase: An ab initio study. *Computational Materials Science*, **113**, pp.148-153.
53. Li, S., Ahuja, R., Barsoum, M.W., Jena, P. and Johansson, B. (2008). Optical properties of $Ti_3SiC_2$ and $Ti_4AlN_3$. *Applied Physics Letters*, **92**(22), p.221907. https://doi.org/10.1063/1.2938862
54. Hossain, M.A., Ali, M.S. and Islam, A.K.M.A. (2012). Rare earth rhodium borides $RRh_3B$ (R= Y, Zr, and Nb): mechanical, thermal and optical properties. *The European Physical Journal B*, **85**(12), p.396.
55. Roknuzzaman, M. and Islam, A.K.M.A. (2012). Theoretical investigations of superconducting MAX phases $Ti_2InX$ (X= C, N). *arXiv preprint arXiv:*1206.4514.
56. Saniz, R., Ye, L.H., Shishidou, T. and Freeman, A.J. (2006). Structural, electronic, and optical properties of $NiAl_3$: first-principles calculations. *Physical Review B*, **74**(1), p.014209.
57. Fox, M. (2002). Optical properties of solids. ISBN 978-O-19850612-6 (paperback), 1-58.
58. Russell, P. (2003). Photonic crystal fibers. *Science*, **299**(5605), pp.358-362. https://doi.org/10.1126/science.1079280

**Citation:** Naefa MJ, and Rahman MA. (2020). First principles study of structural, elastic, electronic and optical features of the non-centrosymmetric superconductors $SrMGe_3$ (Where M= Ir, Pt, and Pd), *Int. J. Mat. Math. Sci.*, **2**(2), 16-28. https://doi.org/10.34104/ijmms.020.016028